JOURNAL OF AIRCRAFT
Vol. 47, No. 6, November–December 2010

Nature of Wakelike and Jetlike Axial Tip Vortex Flows

T. Lee* and J. Pereira†
McGill University, Montreal, Quebec H3A 2K6, Canada

DOI: 10.2514/1.C000225

The mechanisms responsible for the wakelike and jetlike axial flows of a tip vortex were investigated experimentally at $Re = 3.07 \times 10^5$. Both square and round tips were tested. Along the wing tip, a pocket of a higher-than-freestream, or jetlike, fluid was continually present, regardless of the tip condition and airfoil angle of attack α. Its maximum velocity increased with α and always exhibited a peak value around the trailing edge. In the near field, this jetlike fluid pocket was entrained by the shear layers and the wing wake, and it resulted in a wakelike axial flow for smaller α. For higher α, the jetlike fluid pocket was, however, surrounded by the shear layers that, in turn, protected it from the destructive effects of the wing wake and remained jetlike. The switchover angle at which the axial flow switched from wakelike to jetlike appeared around 7 deg, regardless of the tip condition, which also coincided with the angle at which the lift-to-drag ratio was a maximum. Finally, the round-tip-produced vortex was more concentrated and had a higher peak tangential velocity and core circulation but a smaller core radius compared with those of the square tip.

Nomenclature

AR	=	aspect ratio, $(2b)^2/S$
b	=	half-wing span
c	=	airfoil chord
C_D	=	total drag coefficient
C_L	=	total lift coefficient
C_{Di}	=	lift-induced drag coefficient, $D_i/\frac{1}{2}\rho u_\infty^2 S$
D_i	=	lift-induced drag
L/D	=	lift-to-drag ratio
Re	=	Reynolds number, cu_∞/ν
r	=	radius
r_c	=	core radius
r_o	=	outer radius
S	=	wing surface area
u, v, w	=	mean axial, transverse, and spanwise flow velocity
u_c	=	core axial flow velocity
$u_{\max}$	=	maximum velocity of fluid pocket
u_∞	=	freestream velocity
x, y, z	=	streamwise, spanwise, and transverse direction
v_θ	=	tangential velocity
$v_{\theta,\text{peak}}$	=	peak tangential velocity
α	=	angle of attack
Γ	=	circulation
Γ_c	=	core circulation
Γ_o	=	total circulation
δ	=	measurement grid resolution
ζ	=	vorticity
ζ_{peak}	=	peak vorticity
ν	=	fluid kinematic viscosity

Introduction

THE characterization and control of wingtip generated tip vortices, due to their hazardous conditions on flight safety and the accompanied lift-induced drag, continues to be a challenge for the aviation industry and aerodynamicists. Extensive studies of tip vortices, in the intermediate and far fields, have been performed by researchers elsewhere. Recently, there has been a greater emergence of studies focusing on the dynamics and roll up of the tip vortex in the near field. It is now known that, in the near field, the core vortex flow parameters are largely affected by the angle of attack α, the distance downstream from the wing leading edge (i.e., x/c), tip shape, airfoil shape, Reynolds number, surface roughness, measurement resolution, and the experimental technique used. It appears that the parameters that most strongly affect tip vortex behavior are α, x/c, tip shape, and grid resolution. Nevertheless, a large scatter in the core vortex flow data, especially the wakelike and jetlike axial flow [1–15] from previous experimental studies, however, was observed.

Corsiglia et al. [2] studied the near-field characteristics of a trailing vortex generated by a blunt-tipped NACA0015 wing at $Re = 9.53 \times 10^5$ and $\alpha = 12°$, with a measurement grid resolution of $\delta = 3.2\%c$, by using triple hot-wire probes. They reported that the core axial velocity u_c was jetlike with $u_c = 1.1$ to $1.2u_\infty$ for $x/c = 1$ to 6, and the u_c could be as high as $1.4u_\infty$ for $x/c < 1.0$, where x was the distance from the wing leading edge. Orloff [3] examined the effect of α on the tip vortex generated behind a square-tipped NACA0015 wing at $x/c = 3$ and $Re = 7 \times 10^5$ by using laser Doppler velocimetry with $\delta = 0.92\%c$. The u_c was found to increase from $0.85u_\infty$ to $1.15u_\infty$, suggesting a possible crossover point between wakelike and jetlike axial flow. This idea of a crossover point was also studied by Brown [4], who showed that the core axial velocity of the tip vortex was a function of the lift-and-profile drag. Also, in essence, the maximum lift-to-drag ratio point should correspond to $u_c/u_\infty \approx 1$. Similar results, in relation to α, were recently obtained by Lee et al. [15] for a square-tipped NACA0015 wing at $x/c = 2.5$ with a grid resolution of $0.63\%c$ by using a seven-hole pressure probe. The magnitude of u_c was observed to vary from $0.81u_\infty$ (i.e., wakelike) to $1.14u_\infty$ (i.e., jetlike) between $\alpha = 2$ to 18°.

A more in-depth tip vortex study was conducted by McAlister and Takahashi [9] by using a NACA0015 wing with both square and round tips at different α and x/c for $Re = 1.5 \times 10^6$ to 2.5×10^6. The Re was found to produce only slight differences in core vortex flow parameters and did not offer any conclusive results. The maximum core axial velocity of $u_c/u_\infty = 1.5$ was found to occur at $x/c = 1.1$ and $\alpha = 12°$. A switchover point in the wakelike and jetlike axial velocity distributions between 4 and 12° was noticed. Also, the round tip created much smoother separation characteristics and, thus, a more concentrated vortex with u_c increasing from $1.43u_\infty$ to $1.50u_\infty$ near the wing trailing edge (i.e., $x/c = 1.1$). The effect of the chord Reynolds number (for $Re = 7.5 \times 10^5$ to 12.5×10^5) on the tip vortex, generated by a NACA0015 wing equipped with both square and round tips, was further studied by Anderson and Lawton [14] by using triple hot-wire probes with $\delta = 0.3\%c$. Their results also showed little variation in the core axial

Received 10 December 2009; revision received 17 August 2010; accepted for publication 20 August 2010.

*Associate Professor, Department of Mechanical Engineering.
†Graduate Research Assistant, Department of Mechanical Engineering.

velocity with Re. Instead, differences in the core axial velocity, in particular, were found to be correlated with the wing circulation; low values of circulation (i.e., an explicitly smaller α) resulted in deficit profiles (i.e., wakelike axial velocities). Anderson and Lawton also found the core axial velocity to be quite sensitive to tip condition. The round-tipped wing resulted in much higher core velocities and smaller core radii. Note that the dependence of u_c on tip condition was also previously investigated by Thompson [5] on a NACA0012 wing equipped with square, round, and bevelled wing tips by using dye and hydrogen bubble visualizations. Thompson reported that the sharpness of the square and bevelled tips caused the flow to separate at the sharp edges, forming secondary and tertiary vortices that merged, creating a messier and more diffused tip vortex. In contrast, the rounded tip only had one separation line, which created a cleaner and more concentrated vortex.

On the other hand, the effect of surface roughness was examined by Francis and Katz [7]. They suggested that the nature of the axial flow was a balance between the Bernoulli effects, hypothesized by Batchelor [16], and the momentum defect present in the wing boundary layer. Thus, at low Reynolds numbers, the boundary layer should have a stronger influence and cause an axial flow deficit, while at high Reynolds numbers, the Bernoulli effects should reign. This boundary-layer momentum deficit theory implies that a larger deficit would occur for a thicker boundary layer. Thus, a thickened, tripped boundary layer should result in a more wakelike flow. The effect of tripping was further studied by Katz and Galdo [8], in which it was concluded that tripping has a very minor effect on the physical dimensions of the vortex. The effects of the size and location of the boundary-layer trip on vortex core parameters were also investigated by Devenport et al. [11] by using a four-wire probe. Boundary-layer trips extending from 0 to 40%c, from 20 to 40%c, and with no trip were tested at $\alpha = 5^\circ$ and $x/c = 10$ on a square-tipped NACA0012 wing at $Re = 5.3 \times 10^5$. A much larger deficit with boundary-layer trip was observed, which also tended to become more pronounced as the width of the trip was increased. All of Devenport et al.'s results showed a deficit velocity profile (i.e., a wakelike axial flow) ranging from $0.805u_\infty$ to $0.915u_\infty$, depending on the airfoil incidence, for $\alpha = 2.5$ to 7.5°. It should be noted that the main contribution in Devenport et al.'s study was, however, related to the quantifications of the meandering of the vortex in both space and time downstream of the wing tip.

Nevertheless, the most extensive study of the tip vortex flowfield, generated by a round-tip NACA0012 wing with $c = 1.2$ m and a half span of $b = 0.9$ m, was undertaken by Chow et al. [12] for $x/c \leq 1.678$ (measured from the wing leading edge) at $Re = 4.6 \times 10^6$ and $\alpha = 10^\circ$ with $\delta = 2\%c$. The boundary-layer transition was fixed at 4%c from the leading edge via a 0.25%c wide trip strip. Detailed mean flowfield measurements were achieved by using a seven-hole probe and were supplemented with turbulence measurements obtained with a triple hot wire. The core axial velocity was found to be jetlike over the entire axial range covered ($x/c = 0.75$ to 1.678), reaching a maximum of $1.77u_\infty$ upstream of the trailing edge at $x/c = 0.995$ and slowly decreasing to $1.69u_\infty$ at $x/c=$ 1.678. Chow et al. attributed these high excesses to a combination of rounding the tip and testing at a much higher Re than previously tested. They also suggested that, in the near field, the vortex meandering had a small influence on the core vortex flow parameters. Ramaprian and Zheng [13] also measured the tip vortex flow, generated behind a square-tipped NACA0015 wing at $Re = 2.25\times 10^5$, by using laser Doppler velocimetry for $x/c = 1.33$ to 4.33 at $\alpha = 5$ and 10°. The axial core velocity was, however, seen to actually increase with downstream distance from $0.68u_\infty$ to $0.78u_\infty$. Also, the deficit (in the axial tip vortex flow) appeared to remain wakelike with $u_c = 0.78u_\infty$ for both $\alpha = 5$ and 10°. The large differences in reported values between their study and that of Chow et al. [12] were suggested to be attributed to Re and surface roughness effects. A more detailed comparison among published data, including the present measurements, is also summarized in Table 1. Also included in Table 1 are the other core vortex flow parameters.

In summary, it has previously been suggested that rounding the wing tip could have a profound effect on the formation and development of the tip vortex and may even be a determining factor for jetlike axial flow. The objective of this experiment was to clarify the mechanisms responsible for the wakelike and jetlike axial flows of a tip vortex generated by a rectangular NACA0012 wing with both square and round tips, both along the tip and in the near field, in a subsonic wind tunnel. The tip vortex flowfields were measured with a miniature seven-hole pressure probe. Force-balance data were also obtained to supplement the flowfield measurements.

Experimental Method

The experiment was conducted in the $0.9 \times 1.2 \times 2.7$ m^3 low-turbulence suction-type wind tunnel in the Aerodynamics Laboratory at McGill University. A rectangular half-wing model, with a NACA0012 profile, with $c = 28$ cm, a semispan of 50.8 cm, and a removable round endcap NC machined out of solid aluminum was used as the test model. The rounded cap, with a NACA0012 profile, had a chord length of 28 cm, a maximum thickness of 12%c, and a

Table 1 Variation of core vortex flow parameters with airfoil profile, AR, Re, tip condition, x/c, α, and δ

Reference	Airfoil (NACA)	AR	Re ($\times 10^5$)	Tip	x/c	α	u_c/u_∞	$v_{\theta,\text{peak}}$ (%u_∞)	r_c (%c)	Γ_c/cu_∞ ($\times 10^{-2}$)	δ (%c)
Chigier and Corsilia [1]	0015	5.33	9.53	[a]	0.25–5	12	1.1–1.4	12–42	1.3–7.1	——	3.2
Corsiglia et al. [2]	0015	5.33	3	[a]	27–165	8	0.8	34	5.3	——	1.5
Orloff [3]	0015	5.33	7	[a]	3	8–12	0.85–1.15	35–56	6.7–8	2.65	0.9
Thompson [5]	0012	3.91	0.68	[ba]	31–36	0–20	<1	——	——	——	——
McAlister and Takahashi [9]	0015	6.6	15,25	[ba]	1.1–5	4, 8, 12	0.8–1.3	30–80	——	——	1.5
Devenport et al. [11]	0012	8.66	5.3	[a]	5–30	5	0.86	26–29	3.3–3.6	5.6–6.9	0.4
				[a]	10	2.5–7.5	0.81–0.92	17–42	1.9–4.5	2–12	0.4
Chow et al. [12]	0012	1.5	46	[b]	0–1.68	10	1.69–1.77	79–107	1.88–3.1	——	2
Ramaprian and Zheng [13]	0015	4	1.8	[a]	4.33	5	0.78	19.2	8	——	0.8
				[a]	1.33–4.33	10	0.68–0.78	40–43	5–6	——	0.8
Anderson and Lawton [14]	0015	1.6	7.5–12.5	[a]	2–3	4–10	0.8–1.16	27–50	1.9–2.4	——	0.3
				[b]	2–3	4–10	0.9–1.45	44–66	1.5–1.85	——	0.3
Lee et al. [15]	0015	5	2.01	[a]	0.5–3	10	0.95–1.05	52–63	6.5–7.5	15–20	0.6
				[a]	2.5	2–18	0.81–1.14	15–70	3–8.5	20–25	0.6
Present data	0012	3.6	3	[a]	5	5	0.88	29	3.8	10.6	0.85
				[b]	5	5	0.89	43	2.6	11.5	0.85
				[a]	10	5	1.12	56	5.5	19.3	0.85
				[b]	10	5	1.14	68	3.5	15	0.85

[a]Square condition.
[b]Round-tip condition.

maximum height of $6\%c$. The endcap was added to the wingtip using double-sided tape and plastering any gaps to provide a smooth tip shape. The wing was mounted vertically at the center of the bottom wall of the test section, and the chord Reynolds number was fixed at 3.07×10^5. The origin of the coordinate system was measured from the leading edge of the wing tip, with x, y, and z aligned with the streamwise, spanwise, and transverse directions, respectively. The boundary layer was tripped using closely spaced 0.5-mm-diam magnet wires, forming a $5\%c$-wide trip strip located at $5\%c$. The mean streamwise u, spanwise v, and transverse w velocity components were measured, both along the tip and in the near field, by using a miniature seven-hole pressure probe, calibrated in situ, with a diameter of 1.8 mm. Seven Honeywell DC005NDR5 differential pressure transducers were used to obtain the mean pressure at each probe hole. To maximize the output range, the pressure signals were amplified five times, simultaneously sampled at a rate of 500 Hz for 10 s, and recorded through a National Instruments NI-6259 16-bit A/D board. Probe traversing was achieved with a custom-built three-axis traverse. Flowfield measurements were obtained at selected cross-stream planes located at $x/c = 0.4, 0.5, 0.6, 0.7, 0.8, 0.9, 1.05, 1.2, 1.5, 2, 3, 4, 5$, and 6 for $\alpha = 5$ and 10°. Measurements at $x/c = 0.9$ and 5 were also made for $\alpha = 4°$, 6 to 9°, and 11 to 15°.

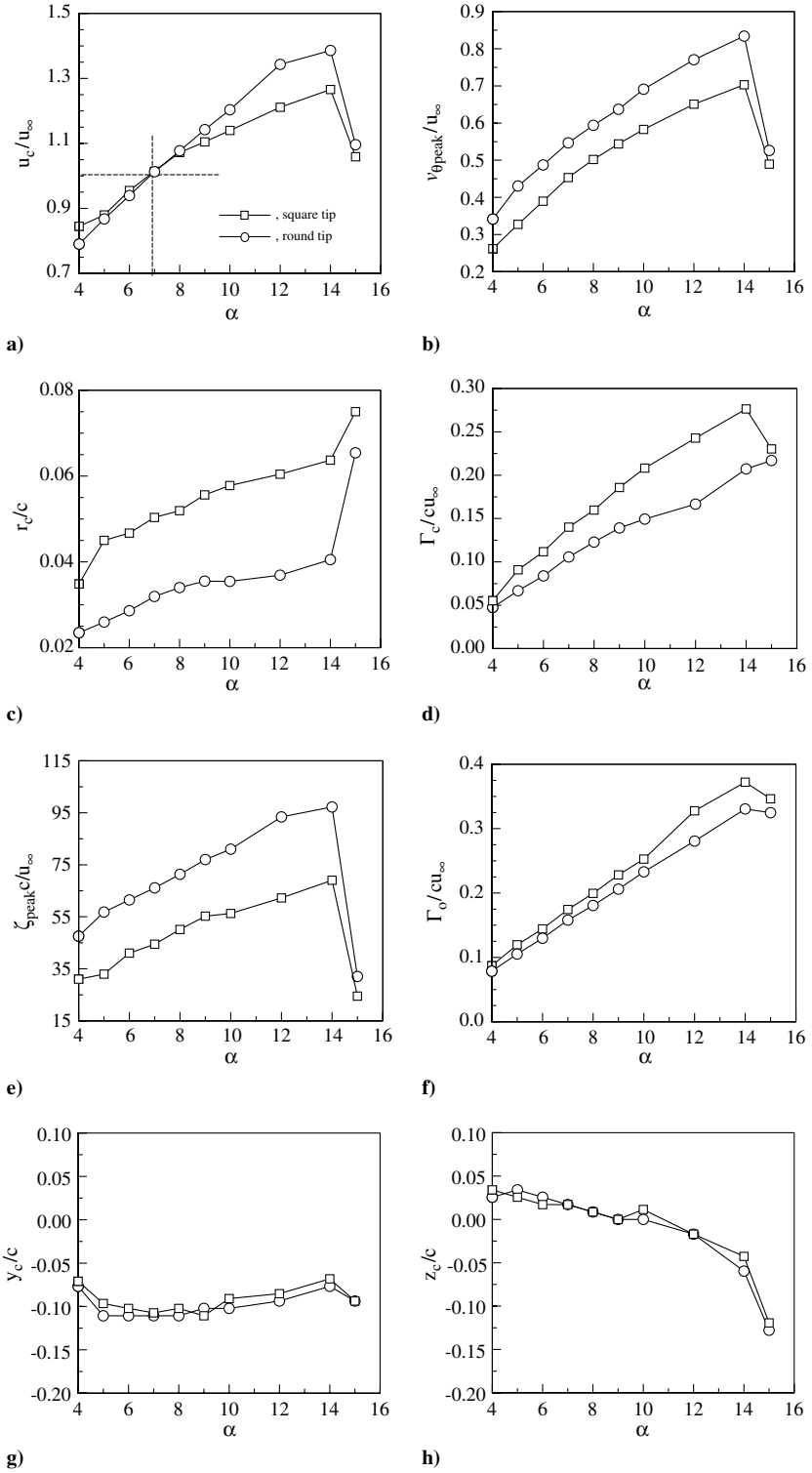

Fig. 1 Variation of critical vortex flow parameters with α at $x/c = 5$ for square and round-tip conditions.

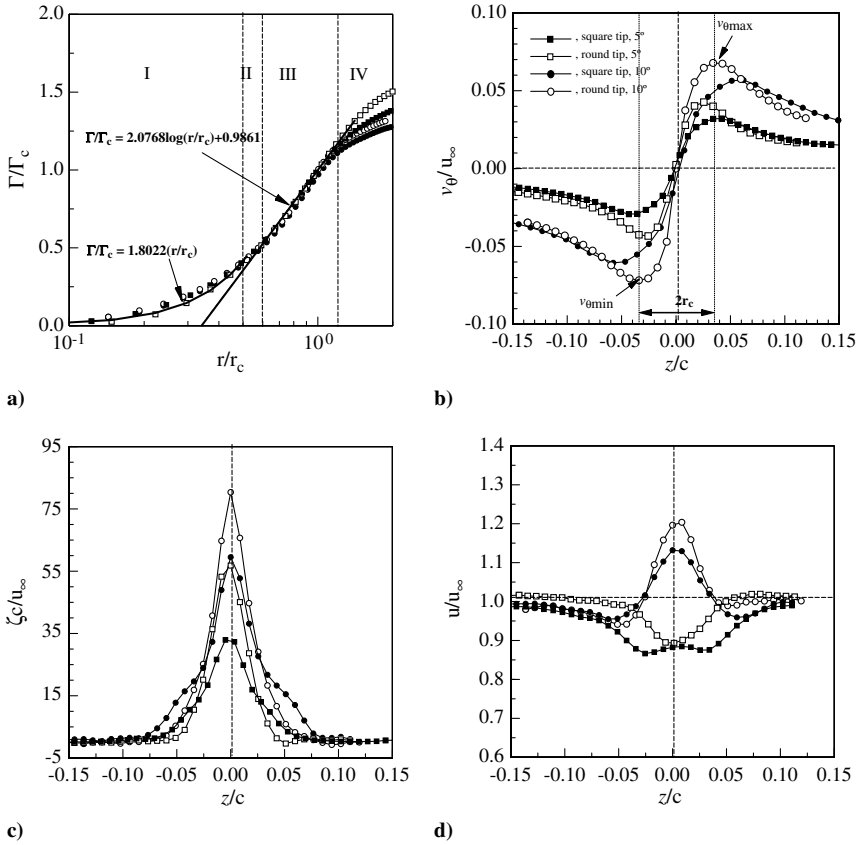

Fig. 2 Typical vortex flow characteristics at $x/c = 5$ for $\alpha = 5$ and 10°: a) radial circulation behavior and distribution of normalized, b) v_θ, c) ζ, and d) u across the vortex center (I: linear region, II: buffer region, III: logarithmic region, and IV: wake region).

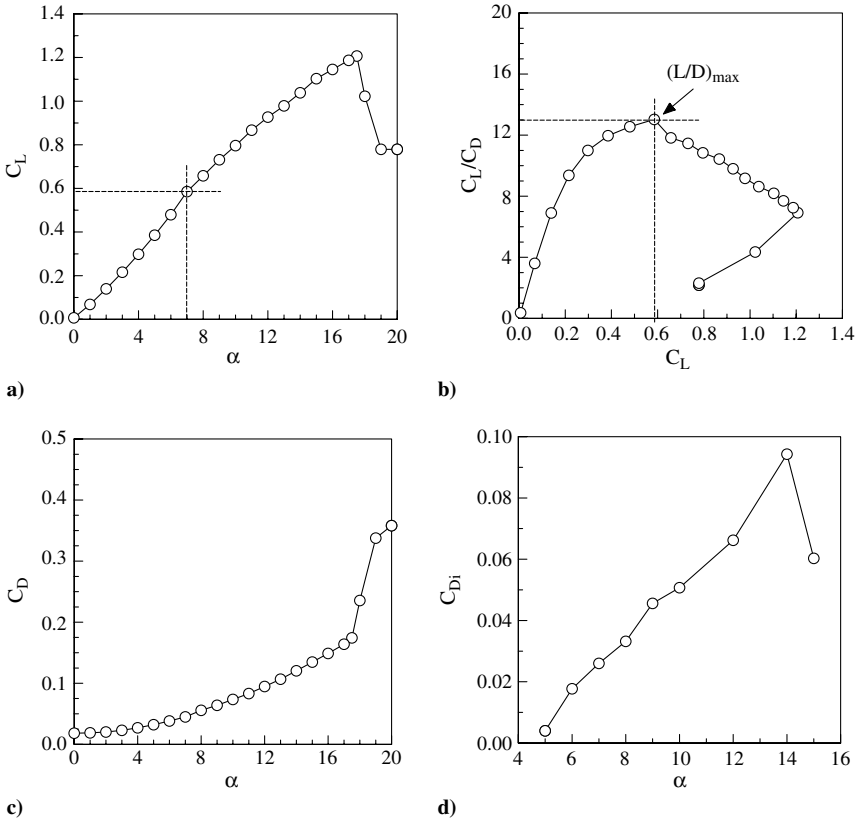

Fig. 3 Aerodynamic characteristics of square-tipped wing at $Re = 3.07 \times 10^5$.

The grid resolution used was 2.4 mm, corresponding to $\delta = 0.85\%c$. The maximum uncertainties are estimated as follows: 2.8% for u, 1.5% for v and w, vorticity of 9%, and core radius of $1\%c$.

The total lift C_L and drag C_D coefficients were obtained by mounting the half-wing model vertically on an external force balance at the same Re. The force-balance calibration was obtained through the application of known weights. The maximum uncertainty in C_L and C_D determinations were ± 0.005 and ± 0.0025, respectively.

Results and Discussion

To better illustrate the mechanism responsible for the wakelike and jetlike axial flows of a vortex, as observed by researchers elsewhere, the variation of the normalized core axial velocity u_c with α at $x/c = 5$ was investigated first and is summarized in Fig. 1a. The $x/c = 5$ downstream location was chosen based on the fact that the core vortex flow parameters, which also include the peak tangential velocity $v_{\theta,\text{peak}}$, and the core radius r_c (defined as the radius at which the tangential velocity v_θ is a maximum) and circulation Γ_c became basically unchanged with x/c for $x/c > 3.5$. For $x/c > 3.5$, the inner flow region of the tip vortex also exhibited a nearly axisymmetric, or self-similar, behavior. The self-similar behavior can be reflected from the radial circulation distribution within the tip cortex core, as shown in Fig. 2a, which was found to follow an $\Gamma(r) \sim r^2$ profile for $r/r_c < 0.4$ (designated by region I) and vary logarithmically for $0.5 < r/r_c < 1.2$ (designated by region III), regardless of the α and the tip condition. This observation is consistent with the findings of Hoffmann and Joubert [17], Moore and Saffman [18], Phillips [19], Ramaprian and Zheng [13], and Lee et al. [15]. The curve-fit equations of regions I and III are also shown in Fig. 2a. The circulation was obtained by summing the vorticity multiplied with the incremental area of the measuring grid. Figure 2a further indicates that, for $r/r_c > 1.4$, $\Gamma(r)$ was, however, found to continue to vary with x/c, suggesting that, for $r > 1.4r_c$, the roll up of the vortex was nearly complete, and there was a slow addition of vorticity to the outer layers of the vortex. The near completion of the vortex development can also be manifested from the nearly axisymmetric distribution in the tangential velocity (with $v_{\theta,\text{peak}} = v_{\theta,\max} \approx |v_{\theta,\min}|$; Fig. 2b) and the Gaussian distribution in the streamwise vorticity ζ across the vortex center (Fig. 2c). The distribution of the mean axial flow u across the vortex center is also presented in Fig. 2d. It should be noted that, even though the overall behavior of v_θ and ζ remained insensitive to the tip condition and the α (except for their peak magnitude, which increased with increasing α) and had a much higher value for the round tip in comparison to the square tip, the axial velocity of the tip vortex was, however, always found to be wakelike for $\alpha = 5°$, while it was always found to be jetlike for $\alpha = 10°$. The round tip only produced a slightly higher core axial velocity u_c at $x/c = 5$ compared with the square tip.

The present measurements also show that, for the square-tipped wing, the core axial vortex flow u_c at $x/c = 5$ was found to increase with the increasing α (see Fig. 1a). A u_c of $0.82u_\infty$ at $\alpha = 4°$ compared with $1.2u_\infty$ at $\alpha = 12°$ was observed. Additionally, a switchover angle at which the core axial flow switched from wakelike (with $u_c < u_\infty$) to jetlike (with $u_c > u_\infty$) appeared around $\alpha = 7°$. This switchover angle was also found to coincide with the angle at which the lift-to-drag ratio was a maximum (see Figs. 3a and 3b), which is in agreement with Brown's [4] hypothesis. The variation of the total drag coefficient C_D ($C_{Dp} + C_{Di}$, where C_{Dp} is the profile drag coefficient, $C_{Di} = D_i/\frac{1}{2}\rho u_\infty^2 S$ is the lift-induced drag coefficient, D_i is the lift-induced drag, ρ is the fluid density, and S is the total wing surface area) with the α of the square-tipped wing at $Re = 3.07 \times 10^5$ is also presented in Fig. 3c. The C_D increased continuously with the increasing α, regardless of the reduction in C_{Dp} resulting from the jetlike axial flow for $\alpha > 7°$, as a consequence of the large increase in the lift-induced drag coefficient (see Fig. 3d). The lift-induced drag was obtained by (as suggested by Brune [20] and Kusunose [21])

$$D_i = \frac{1}{2}\rho_\infty \iint_{S_\zeta} \psi\zeta \,\mathrm{d}y\,\mathrm{d}z - \frac{1}{2}\rho_\infty \iint_{S_1} \phi\sigma \,\mathrm{d}y\,\mathrm{d}z \tag{1}$$

where $\zeta = \partial w/\partial y - \partial v/\partial z$ is the streamwise vorticity, the surface S_ζ is the region within S_1 where the vorticity is nonzero, and $\sigma = \partial v/\partial y + \partial w/\partial z = -\partial u/\partial x$ is a source term that is small outside the viscous wake. Furthermore, similar to the observed increase in u_c with α, the values of $v_{\theta,\text{peak}}$, r_c, Γ_c, and ζ_{peak} of the square-tipped wing were also found to increase as α was increased, regardless of the tip condition (Figs. 1b–1e). Figures 1b–1e further indicate that, at the same x/c (5) and α, the round-tipped wing, however, generated a more concentrated and strengthened tip vortex with a greatly increased $v_{\theta,\text{peak}}$ and ζ_{peak} but a much smaller r_c compared with those of the square tip, which is in agreement with the observations made by Chow et al. [12]. The core circulation, however, was of a reduced magnitude compared with the square tip (Fig. 1d), mainly due to the significantly reduced core radius. Moreover, a small discrepancy in the total circulation Γ_o was also noticed between the two tip conditions (Fig. 1f). The location of the vortex center, of both the square and round-tip conditions, as a function of the angle of attack at $x/c = 5$ is summarized in Figs. 1g and 1h. There appeared to be very little difference in vortex trajectory between square and round tips.

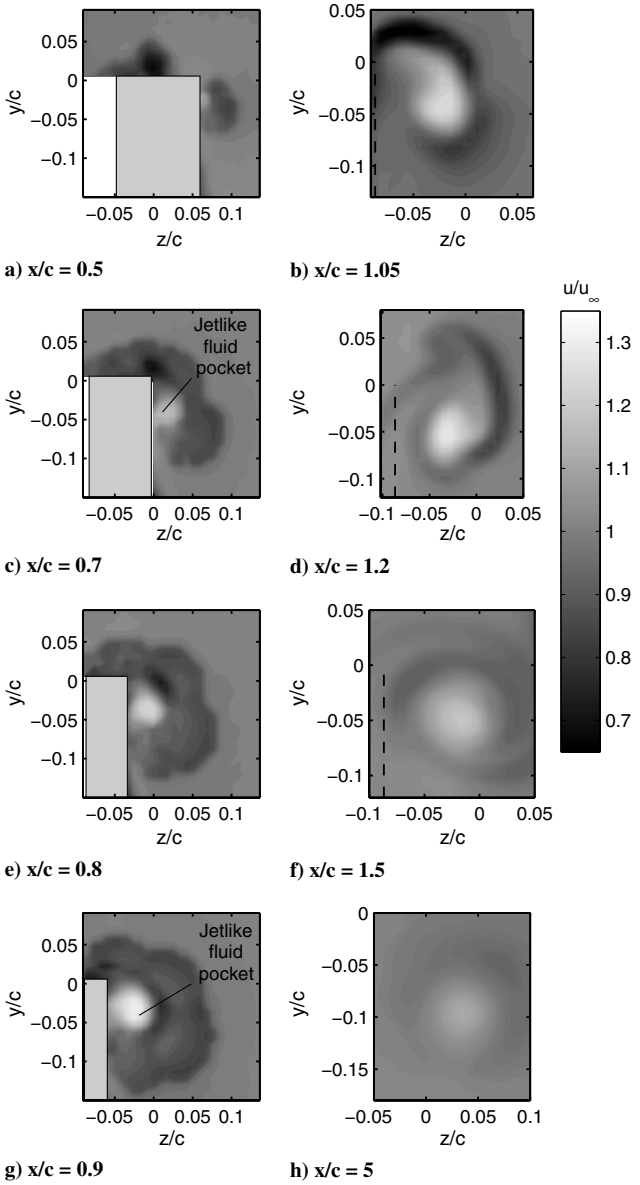

Fig. 4 Representative normalized isoaxial flow contours along the square tip and in the near field for $\alpha = 10°$.

Figure 1a further reveals that there was a minor decrease in the core axial flow velocity at low α, compared with the square tip. At high α, the u_c of the round-tipped wing increased above the square-tip value. This discrepancy also widened as α was increased. More important, the switchover angle was not affected by the tip condition. That is, the tip condition only influenced the magnitude of u_c, to a lesser extent, but not the nature of the wakelike or jetlike axial flow. It is, therefore, surmised that, in addition to the airfoil incidence, whether or not the axial velocity in the tip vortex becomes wakelike or jetlike should also be a function of the streamwise distance. To elucidate the effects of the streamwise distance (i.e., x/c) on the wakelike and jetlike axial flows observed in the near field (as discussed in Fig. 1a), the normalized isoaxial velocity u/u_∞ and isovorticity $\zeta c/u_\infty$ contours, both along the tip (for $0.4 \leq x/c \leq 0.9$) and in the near field (for $1.05 \leq x/c \leq 5$), for both square- and round-tipped wings, positioned at $\alpha = 10$ and 5°, were examined.

Figures 4a, 4c, 4e, 4g, 5a, 5c, 5e, and 5g display the selected iso-u/u_∞ and iso-$\zeta c/u_\infty$ contours along the square tip (at $x/c = 0.5$, 0.7, 0.8, and 0.9) for $\alpha = 10°$. At $x/c = 0.5$, the rolling up of the separated shear layers around the square tip and the presence of multiple secondary vortices and the main vortex can be clearly seen (Fig. 5a). Also, as the shear layer separated, it entrained some fluid from the freestream, rendering a small pocket of jetlike fluid (i.e., higher-than-freestream fluid) with a maximum axial velocity $u_{\max}$ of $1.12u_\infty$ (see Fig. 4a). The size and the maximum velocity of this pocket of fluid and the strength of the main vortex, fed by the vorticity supply from the secondary vortices, continued to increase as it progressed downstream along the tip (Figs. 4c and 5c). At $x/c = 0.8$ (Fig. 4e), the large rotational velocity associated with this roll up drove the shear layers to reattach to the wing upper surface, causing the shear layers to completely surround this pocket with a $u_{\max}$ of $1.24u_\infty$. The rotational velocity associated with the rolled-up shear layer increased as the roll up continued and, based on Batchelor's [16] argument, this created a region of low pressure that further accelerated the freestream flow, causing it to become more jetlike along the square tip. An $u_{\max}$ of $1.36u_\infty$ was noticed at $x/c = 0.9$ (Fig. 4g). Meanwhile, as the $u_{\max}$ was gaining strength, the multiple secondary vortices were wrapping around the main vortex, which eventually merged and formed a single vortex as it progressed down the chord (see Figs. 5c, 5e, and 5g). The change in the normalized $u_{\max}$ and ζ_{peak} (of the main vortex) along the square tip for $\alpha = 10°$ is summarized in Figs. 6a and 6b, respectively. Figures 6a and 6b show that both $u_{\max}$ and ζ_{peak} increased along the tip and reached a local maximum around the wing trailing edge, regardless of the tip condition. The round-tipped wing, however, produced a slightly lower $u_{\max}$ but a much higher ζ_{peak} along the tip compared with the square tip.

In the near field (for $x/c \geq 1.05$) behind the square-tipped wing, the jetlike axial flow was surrounded by the shear layers, which acted almost like a shield, preventing the low-momentum wake from infiltrating the core flow and decelerating it (see Figs. 4b, 4d, 4f, and 5h). Dashed lines denote the position of the wing trailing edge. As a result, the jetlike flow was able to persist for a much longer amount of time (i.e., up to $x/c = 5$ tested; Fig. 4h), although the magnitude of

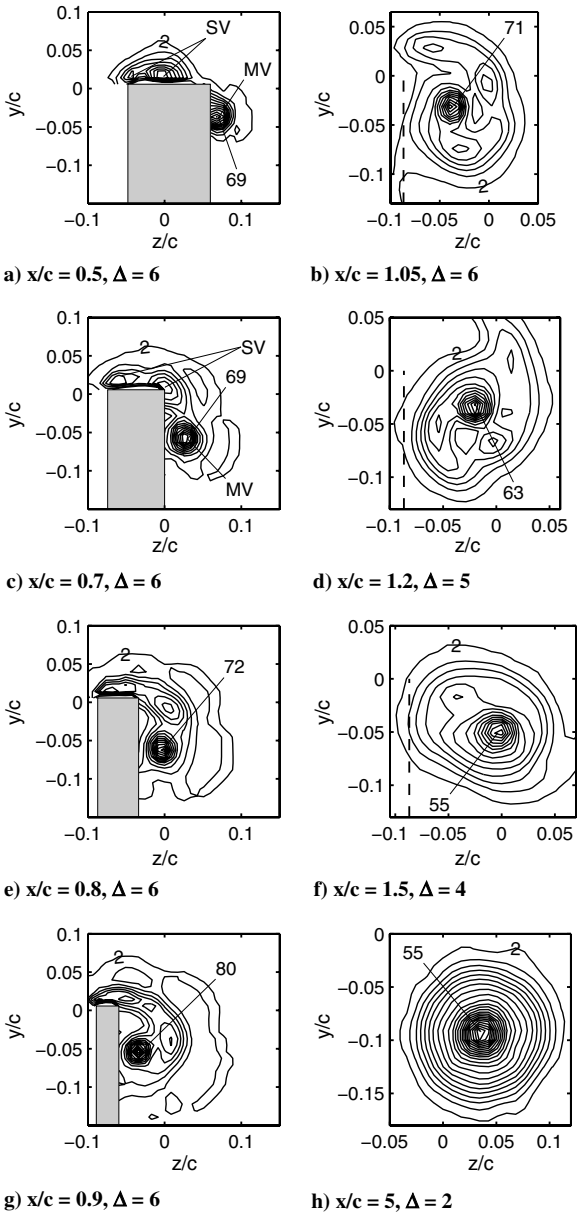

Fig. 5 Representative normalized isovorticity contours along the square tip and in the near field for $\alpha = 10°$ ($\Delta = \zeta c/u_\infty$ indicates increment levels, and SV and MV denote secondary vortices and main vortex, respectively).

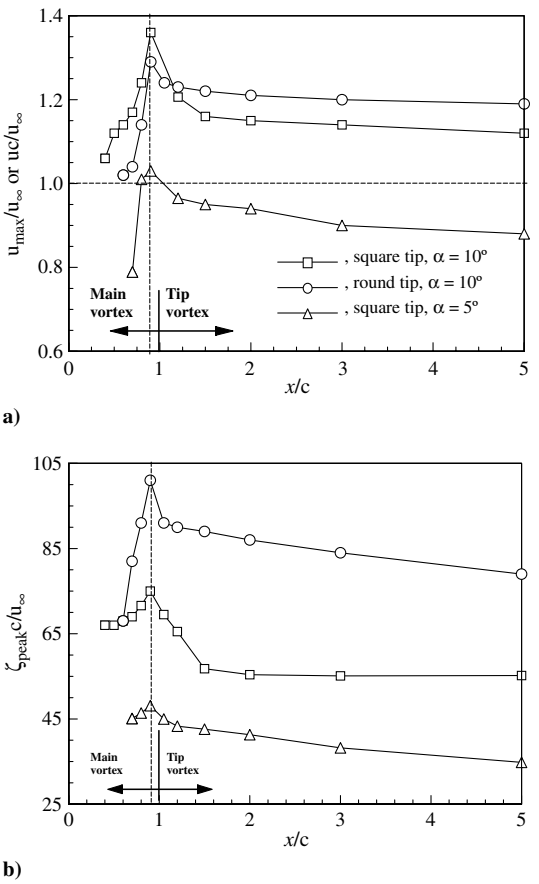

Fig. 6 Variation of normalized $u_{\max}$, u_c, and ζ_{peak} with x/c at $\alpha = 5$ and 10° for both square and round tips.

the jet did slowly decrease with downstream distance (see also Fig. 6a), as a result of the influence of both the wing's wake and viscous diffusion. A core axial velocity u_c of $1.25u_\infty$ at $x/c = 1.05$ and $1.14u_\infty$ at $x/c = 5$ for $\alpha = 10°$ was observed. Note also the rather steep drop in the core axial velocity and ζ_{peak} (of the tip vortex) immediately downstream of the wing trailing edge at $x/c = 1.05$ (Figs. 4b, 5b, and 6a). Meanwhile, the iso-$\zeta c/u_\infty$ contours were exhibiting an asymmetric, or developing, pattern at this measuring station ($x/c = 1.05$). Further downstream of the wing, the tangential velocity and vorticity distributions were attaining axisymmetry, and the axial velocity deficit was reducing (see, for example, Figs. 5d and 5f). The degree of axisymmetry became more pronounced with the downstream distance. For $x/c > 3$ (Fig. 5h), the inner flow region of the tip vortex exhibited a near axisymmetry, as discussed earlier in Figs. 2a–2c. The variation of u_c and ζ_{peak} of the tip vortex with x/c for $1.05 < x/c \leq 5$ at $\alpha = 10°$ is also summarized in Fig. 6. Both u_c and ζ_{peak} were found to decrease with downstream distance, regardless of the tip condition.

The present measurements further reveal that, in comparison to the square-tipped wing at $\alpha = 10°$, the round tip led to the formation of a more concentrated and greatly strengthened main vortex and secondary vortices (see also Figs. 7a and 7c) but a slightly lowered u_{max} (see also Figs. 7b and 7d), compared with the square tip (Figs. 5e, 5g, 4e, and 4g). As hypothesized by Chow et al. [12], this more concentrated vortex is a result of a single separation line along the tip. The overall behavior of the various vortical flow patterns along the tip, however, was not affected by the tip condition. In the near field, there was a minor increase in the jetlike axial flow compared with the square tip (see also Figs. 4b, 4h, 7f, and 7h). A greatly increased ζ_{peak} was, however, observed behind the round tip (Figs. 7e and 7g) compared with that of the square tip (Figs. 5b and 5h). As stated earlier in Figs. 1b–1d, the more concentrated tip vortex, generated behind the round-tipped wing, resulted in a higher tangential velocity but a smaller core radius and circulation, compared with the square tip. An $u_{max} = 1.29u_\infty$ and $u_c = 1.2u_\infty$ (with $\zeta_{peak}c/u_\infty = 101$ and 80) at $x/c = 0.9$ and 5, respectively, for $\alpha = 10°$ of the round tip compared with $1.36u_\infty$ and $1.14u_\infty$ (with $\zeta_{peak}c/u_\infty = 71$ and 55) of the square tip was noticed (Figs. 6a and 6b). This suggests that the tip shape may greatly influence the strength of the jet, but it is not the cause of the jetlike flow. It is, therefore, believed that it was not just the airfoil incidence but also the tip vortex's interaction with the wing wake that would ultimately determine the nature of the axial flow (i.e., wakelike or jetlike) at a certain downstream location behind the wing.

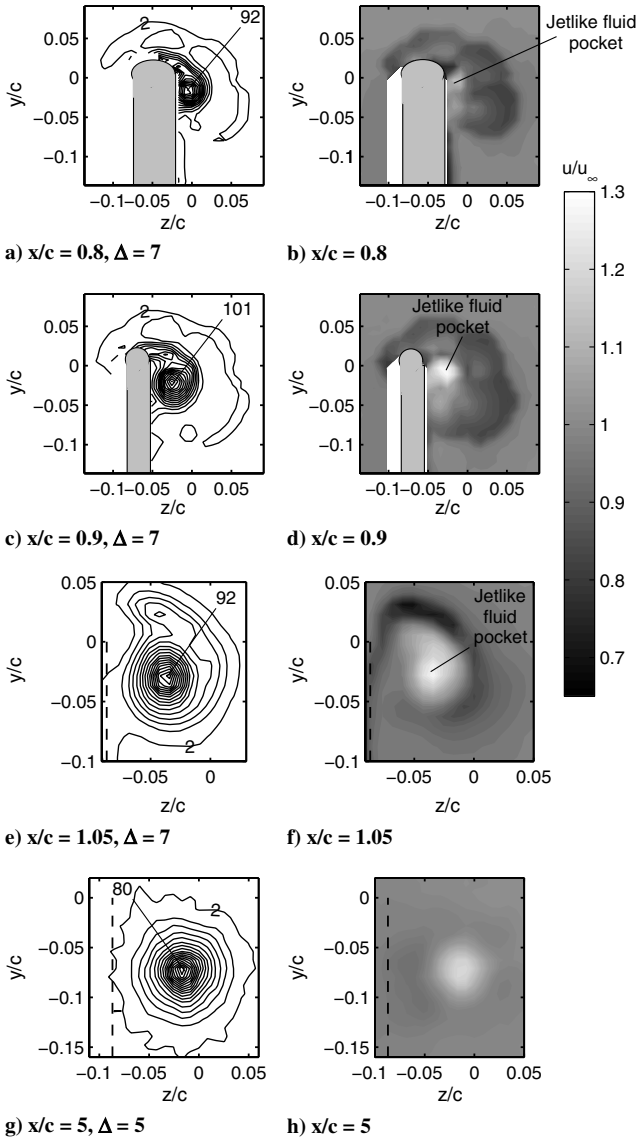

Fig. 7 Round-tip results for $\alpha = 10°$: a, c, e, and g) iso-$\zeta c/u_\infty$ contours; and b, d, f, and h) iso-u/u_∞ contours ($\Delta = \zeta c/u_\infty$ indicates increment levels).

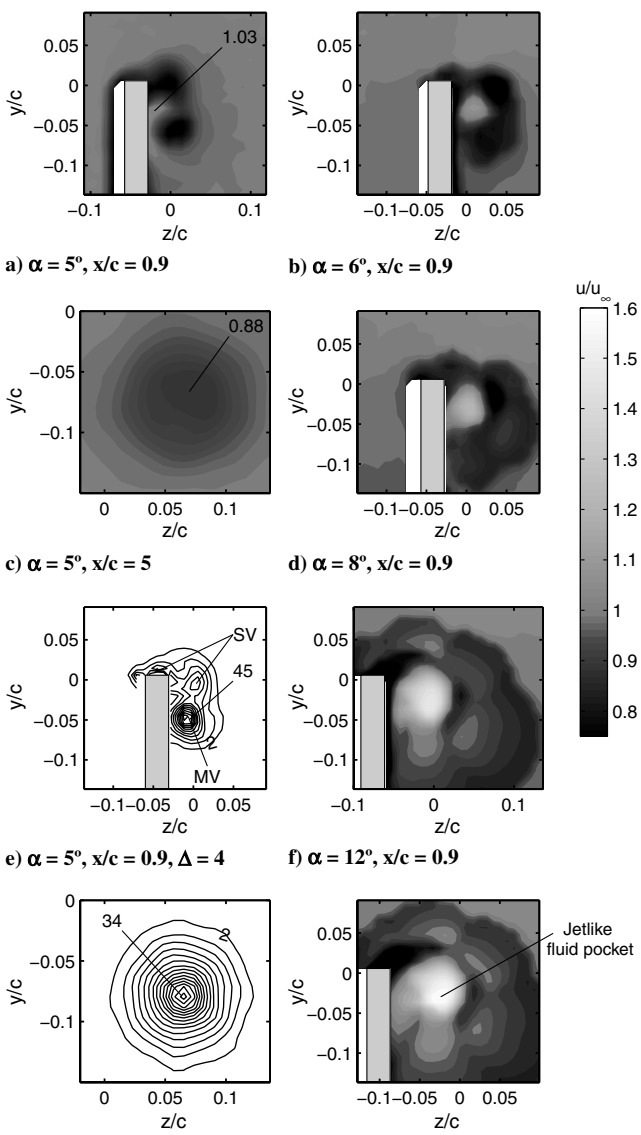

Fig. 8 Contours at selected α and x/c: a–d, f, and h) iso-u/u_∞ contours; and e and g) iso-$\zeta c/u_\infty$ contours ($\Delta = \zeta c/u_\infty$ indicates increment levels).

To further reinforce the observation of the higher-than-freestream fluid pocket along the wing tip and its subsequent development in the near field at $\alpha = 10°$, the effects of varying the angle of attack, as opposed to Fig. 4 where the angle of attack was fixed at 10°, on the iso-u/u_∞ and iso-$\zeta c/u_\infty$ contours (along the tip and in the near field) for $\alpha = 4$ to 9° and 11 to 14° were also documented. A similar jetlike fluid pocket was also observed for the $\alpha = 5°$ case. A weaker jet flow of $u_{\max} = 1.03u_\infty$ at $x/c = 0.9$ for $\alpha = 5°$, compared with $u_{\max} = 1.36u_\infty$ for $\alpha = 10°$, however, was observed for the square-tipped wing (Fig. 8a), which was not entrained until the trailing edge was passed. When it was finally entrained, there was no surrounding shear layer to protect it from the wake, and the wake was then able to quickly infiltrate and dwarf the excess at the center. This resulted in a wakelike flow with a u_c of $0.88u_\infty$ at $x/c = 5$ (Fig. 8c; compared with $1.14u_\infty$ at the same downstream distance for $\alpha = 10°$). The variation of the normalized $u_{\max}$, u_c, and ζ_{peak} with x/c of the square-tipped wing, which exhibited a similar trend to that of $\alpha = 10°$, is also summarized in Figs. 6a and 6b. The corresponding iso-$\zeta c/u_\infty$ contours at $x/c = 0.9$ and 5 for $\alpha = 5°$ are also presented in Figs. 8e and 8g. Finally, the presence of the fluid pocket and its maximum velocity at different α was also examined for $x/c = 0.9$. Selected iso-u/u_∞ for $\alpha = 6$, 8, 12, and 14° are presented in Figs. 8b, 8d, 8f, and 8h. The variation of normalized $u_{\max}$ and ζ_{peak} at $x/c = 0.9$ with α is summarized in Fig. 9. Figure 8, together with Fig. 9, clearly shows that, regardless of the angle of attack, a $u_{\max} > u_\infty$ was persistently noticed at $x/c = 0.9$. In contrast, the core axial velocity was wakelike for $\alpha > 7°$, while it was jetlike for $\alpha > 7°$ in the near field (as shown in Fig. 1a). Figure 9a further reveals that the higher the α, the larger the $u_{\max}$, regardless of the tip condition. The round tip had a slightly higher $u_{\max}$ for all α tested. The main vortex generated along the round tip, however, had a much higher ζ_{peak} than the square tip (Fig. 9b). In combination with Fig. 1a, it is evident that, for $\alpha > 7°$, the low-momentum fluid and the associated high level of wake turbulence was able to access the jetlike pocket of fluid developed upstream along the tip, causing the jetlike fluid to quickly dissipate and become wakelike in the near field. For $\alpha > 7°$, the observed jetlike fluid pocket along the tip, however, prevailed in the near wake with a reduced magnitude.

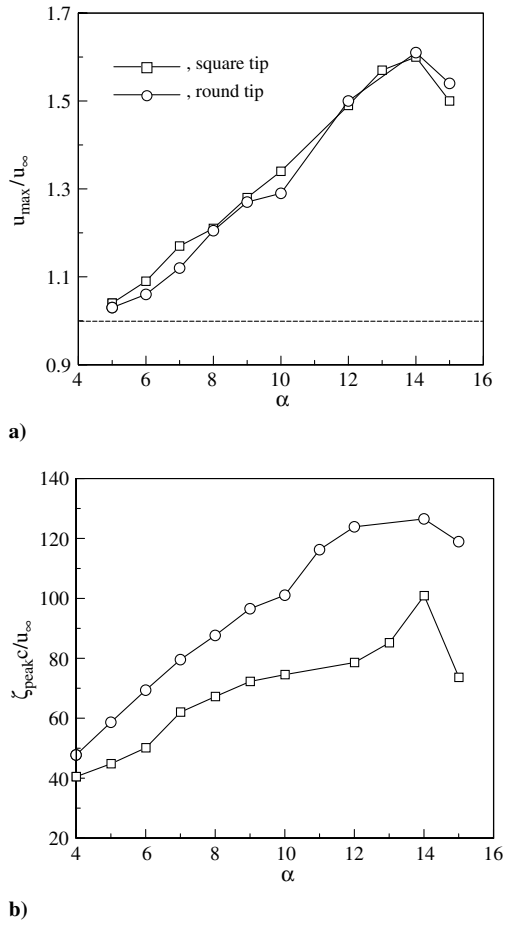

Fig. 9 Variation of normalized $u_{\max}$ and ζ_{peak} with α at $x/c = 0.9$.

Conclusions

The mechanisms behind the observed wakelike and jetlike axial flows of a tip vortex, generated behind a rectangular NACA0015 wing with transition fixed at 5%c, were investigated at $Re = 3.07 \times 10^5$. Both square and round-tip conditions were tested. Along the wing tip, a pocket of a higher-than-freestream, or jetlike, fluid was persistently observed, regardless of the tip condition and the angle of attack. Its maximum velocity was found to increase with the angle of attack and always exhibited a local peak around the wing trailing edge. For smaller angles of attack, this pocket of jetlike fluid was entrained by the shear layers and the wing wake, and thus rendered a wakelike axial flow as it progressed downstream of the wing trailing edge. For higher angles of attack, the jetlike fluid pocket was, however, surrounded by the shear layers that, in turn, protected it from the destructive effects of the wing wake. As such, it took much longer for the wake to decrease the strength of the jetlike axial flow. The jetlike core originated from freestream fluid thus persisted. The switchover angle at which the mean axial vortex flow switched from wakelike to jetlike appeared around 7°, regardless of the tip condition, which also coincided with the angle at which the maximum lift-to-drag ratio was observed. In short, the tip shape may greatly influence the strength of the jet, but it is not the cause of the jetlike flow. Also, it was not just the airfoil angle of attack but also the tip vortex interaction with the wing wake that will ultimately determine the wakelike or jetlike nature of the axial flow at a certain downstream location in the near field. Finally, the round-tipped wing produced a more concentrated tip vortex with a slightly stronger axial flow and a higher peak tangential velocity but a smaller core radius and circulation compared with the square-tipped wing.

References

[1] Chigier, N. A., and Corsiglia, V. R., "Tip Vortices-Velocity Distributions," NASA TM X-62-087, 1971.

[2] Corsiglia, V. R., Schwind, R. G., and Chigier, N. A., "Rapid Scanning Three-Dimensional Hot-Wire Anemometer Surveys of Wing Tip Vortices," *Journal of Aircraft*, Vol. 10, No. 12, 1973, pp. 752–757. doi:10.2514/3.60301

[3] Orloff, K. L., "Trailing Vortex Wind-Tunnel Diagnostics with a Laser Velocimeter," *Journal of Aircraft*, Vol. 11, No. 8, 1974, pp. 477–482. doi:10.2514/3.60371

[4] Brown, C. E., "Aerodynamics of Wake Vortices," *AIAA Journal*, Vol. 11, No. 4, 1973, pp. 531–536. doi:10.2514/3.6781

[5] Thompson, D. H., "Experimental Study of Axial Flow in Wing Tip Vortices," *Journal of Aircraft*, Vol. 12, No. 11, 1975, pp. 910–911. doi:10.2514/3.44500

[6] Francis, M. S., and Kennedy, D. A., "Formation of a Trailing Vortex," *Journal of Aircraft*, Vol. 16, No. 3, 1979, pp. 148–154. doi:10.2514/3.58498

[7] Francis, T. B., and Katz, J., "Observations on the Development of a Tip Vortex on a Rectangular Hydrofoil," *Journal of Fluids Engineering*, Vol. 110, No. 2, 1988, pp. 208–215. doi:10.1115/1.3243536

[8] Katz, J., and Galdo, J., "Effect of Roughness on Rollup of Tip Vortices on a Rectangular Hydrofoil," *Journal of Aircraft*, Vol. 26, No. 3, 1989, pp. 247–253. doi:10.2514/3.45753

[9] McAlister, K., and Takahashi, R., "NACA0015 Wing Pressure and Trailing Vortex Measurements," NASA TP 3151, 1991.

[10] Green, S., and Acosta, A., "Unsteady Flow in Trailing Vortices," *Journal of Fluid Mechanics*, Vol. 227, 1991, pp. 107–134. doi:10.1017/S0022112091000058

[11] Devenport, W. J., Rife, M. C., Liapis, S. I., and Follin, G. J., "The Structure and Development of a Wing-Tip Vortex," *Journal of Fluid Mechanics*, Vol. 312, 1996, pp. 67–106. doi:10.1017/S0022112096001929

[12] Chow, J. S., Zilliac, G. G., and Bradshaw, P., "Mean and Turbulence Measurements in the Near Field of a Wingtip Vortex," *AIAA Journal*,

Vol. 35, No. 10, 1997, pp. 1561–1567.
doi:10.2514/2.1

[13] Ramaprian, B., and Zheng, Y., "Measurements in Rollup Region of the Tip Vortex from a Rectangular Wing," *AIAA Journal*, Vol. 35, No. 12, 1997, pp. 1837–1843.
doi:10.2514/2.59

[14] Anderson, E. A., and Lawton, T. A., "Correlation Between Vortex Strength and Axial Velocity in a Trailing Vortex," *Journal of Aircraft*, Vol. 40, No. 4, 2003, pp. 699–704.
doi:10.2514/2.3148

[15] Lee, T., Birch, D., Mokhtarian, F., and Kafayeke, F., "Structure and Induced Drag of a Tip Vortex," *Journal of Aircraft*, Vol. 41, No. 5, 2004, pp. 1138–1145.
doi:10.2514/1.2707

[16] Batchelor, G. K., "Axial Flow in Trailing Line Vortices," *Journal of Fluid Mechanics*, Vol. 20, No. 4, 1964, pp. 645–658.
doi:10.1017/S0022112064001446

[17] Hoffmann, E. R., and Joubert, P. N., "Turbulent Line Vortices," *Journal of Fluid Mechanics*, Vol. 16, No. 3, 1963, pp. 395–411.
doi:10.1017/S0022112063000859

[18] Moore, D. W., and Saffman, P. G., "Axial Flow in Laminar Trailing Vortices," *Proceedings of the Royal Society of London*, Vol. 333, No. 1595, 1973, pp. 491–508.
doi:10.1098/rspa.1973.0075

[19] Phillips, W. R. C., "The Turbulent Trailing Vortex During Roll-Up," *Journal of Fluid Mechanics*, Vol. 105, 1981, pp. 451–467.
doi:10.1017/S0022112081003285

[20] Brune, G. W., "Quantitative Low-Speed Wake Surveys," *Journal of Aircraft*, Vol. 31, No. 2, 1994, pp. 249–255.
doi:10.2514/3.46481

[21] Kusunose, K., "Drag Reduction Based on a Wake-Integral Method," AIAA Paper 1998-2723, 1998.